

# OPTIMAL LOW-THRUST ORBITAL TRANSFERS AROUND A ROTATING NON-SPHERICAL BODY

Gregory J. Whiffen\*

The NASA Discovery Program mission named DAWN will launch in 2006 to orbit the two giant asteroids Vesta and Ceres. The DAWN spacecraft will use solar-electric propulsion for both the inter-planetary cruise and orbital operations at each asteroid. A method is required to design low-thrust orbital transfers between the science orbits given the complex gravity fields of both asteroids. This paper describes a technique for computing optimal low-thrust transfers in an arbitrarily complex, gravity field of a rotating body. Optimal transfers involving point mass models are compared to optimal transfers in increasingly complex gravity fields. The method is applied to a transfer between a high orbit and a low orbit with a plane change around the Asteroid Vesta using real mission constraints. Vesta's gravity is modeled with a harmonic expansion of order twenty. The Static/Dynamic Control algorithm is used to solve the optimal control problem.

## INTRODUCTION

The NASA Discovery Program mission named DAWN will be launched in 2006 to orbit the two giant asteroids Vesta and Ceres. The two asteroids are so large (530 km and 960 km in diameter, respectively) that they are often referred to as "protoplanets". Both Vesta and Ceres orbit the Sun in the asteroid belt between Mars and Jupiter. Vesta and Ceres are baby-planets whose growth was disrupted by the formation of Jupiter. Vesta and Ceres have different characteristics and formed at different distances from the Sun. Vesta orbits the Sun at approximately 2.3 A.U. while Ceres' orbit extends out to nearly 3 A.U. Vesta has evolved (differentiated) and it is dry. Ceres, in contrast, is primitive and icy.

The DAWN spacecraft will use solar-electric propulsion for the inter-planetary cruise, asteroid capture, and orbital operations at each asteroid. Several science orbits are planned at each asteroid. Low-thrust control combined with the complex gravity of a rotating asteroid results in a new and challenging design problem. Optimizing low-thrust trajectories is well known to be inherently difficult. Accounting for the complex gravitational field further compounds the optimization complexity.

A method is required to design low-thrust orbital transfers at each asteroid. Existing techniques for computing optimal low-thrust orbital transfers do not account for highly non-spherical gravity<sup>1,9</sup>. Orbital motion near asteroids is not accurately described by classical theories for motion around spheroidal (oblate) bodies. In general, numerical integration is required to adequately resolve the motion of a satellite orbiting near an asteroid.

The question of orbital stability around asteroids has been investigated numerically<sup>2</sup>. Generally, science orbits will be selected that are relatively stable (requiring little or no station keeping).

---

\*Senior member of the Engineering Staff, Navigation and Mission Design Section, Jet Propulsion Laboratory, California Institute of Technology, Pasadena, CA 91109

However, transfers between science orbits may not be able to avoid passing through both unstable orbital states and stable states with widely oscillating classical elements. This is not entirely bad. A desirable aspect of these intermediate orbital states is that they result in radical changes in the orbit in a short time or for little propellant cost. If these states are selected properly, then a desired orbital transfer can be achieved very quickly and efficiently. This idea is not new, it has been proposed in the context of asteroids and 3-body systems. The idea is to use adjacent stable and unstable manifolds of (quasi-) periodic orbits to create efficient orbital transfers<sup>3</sup>. However, it is not always clear how to implement this idea. Important families of orbital states can easily remain undiscovered.

Rather than try to discover and piece together various orbital families, a different approach is developed in this paper. An optimal control problem is formulated and solved to minimize the propellant required to achieve an arbitrary orbital transfer around an asteroid. If the problem is solved correctly, then the resulting trajectory will use an optimal sequence of stable and unstable orbital states to achieve the desired end state. The optimal sequence of stable and unstable orbital states occur during coasting (thrust off) phases. Since the mathematical objective is to minimize propellant usage, thrusting (which is minimized) represents transfers between *adjacent* stable/unstable orbital states. Therefore, the goal of finding and stringing together highly efficient stable/unstable orbital states to reach some goal can be achieved in a single optimization step. Once an optimal transfer is computed, an investigation of the trajectory can yield many insights.

In order for an optimal control approach to work, the optimal control formulation must not omit any of the dynamical complexity of the problem. For example, the gravitational field cannot be simplified to reduce the computational effort or improve algorithm convergence. Clearly, a highly robust optimization method is required. The optimization algorithm called Static/Dynamic Control<sup>4</sup> (SDC) was selected due to its unusual robustness and ability to solve highly nonlinear dynamic problems. SDC is a general, second order derivative-based optimal control method. Solutions obtained with SDC satisfy both the necessary and sufficient conditions of optimality. SDC has been successfully applied to N-body point mass gravity models<sup>5,6,7,8</sup>. This paper demonstrates that SDC analysis can be extended to gravity fields that are modeled with a high order harmonic expansions.

## APPROACH

The technique used for computing optimal low-thrust transfers for an arbitrarily complex, rotating gravity field is described in this section. In the next section, optimal transfers involving point mass models and increasingly complex gravity fields are compared. Finally, the method is applied to a transfer between a high orbit and a low orbit with a plane change around the asteroid Vesta. Vesta's gravity is modeled with a harmonic expansion of order twenty.

### Optimal Control Formulation of the Low-Thrust Asteroid Problem

The problem of minimizing the total propellant required to achieve a general orbital transfer is formulated as the following general, non-linear optimal control problem:

$$J^* = \min_{v(t), w} \int_{t_0}^{t_N} F(x(t), v(t), w, t) dt + \sum_{i=1}^N G_i(x(t_i), u_i, w, t_i), \quad (1)$$

subject to a state equation of the form

$$\frac{dx(t)}{dt} = T(x(t), v(t), w, t), \quad (2)$$

and an initial condition of the form

$$x(t_0) = \Gamma(w). \quad (3)$$

The functions  $F$  (accumulated objective) and  $G$  (point-in-time objectives) are user selected, once continuously differentiable objective functions. The number of point-in-time objective functions  $N$  is user selectable; the function  $T$  represents the physical interactions; and the function  $\Gamma$  returns the initial system state.

There are three classes of variables: state variables  $x(t)$ , dynamic control variables  $v(t)$ , and static control variables  $w$ . The components of the state vector  $x(t)$  are defined in a locally inertial frame as follows,

$$x(t) = \begin{bmatrix} x_1(t) \\ x_2(t) \\ x_3(t) \\ x_4(t) \\ x_5(t) \\ x_6(t) \\ x_7(t) \end{bmatrix} = \begin{bmatrix} x \text{ coordinate of spacecraft} \\ y \text{ coordinate of spacecraft} \\ z \text{ coordinate of spacecraft} \\ x \text{ velocity of spacecraft} \\ y \text{ velocity of spacecraft} \\ z \text{ velocity of spacecraft} \\ \text{mass of the spacecraft.} \end{bmatrix} \quad (4)$$

The dynamic and static control vectors  $v(t)$  and  $w$  are defined to be

$$v(t) = \begin{bmatrix} v_1(t) \\ v_2(t) \\ v_3(t) \end{bmatrix} = \begin{bmatrix} x \text{ thrust component} \\ y \text{ thrust component} \\ z \text{ thrust component,} \end{bmatrix} \quad w = \begin{bmatrix} w_1 \\ w_2 \end{bmatrix} = \begin{bmatrix} \text{transfer start} \\ \text{total flight time.} \end{bmatrix} \quad (5)$$

The equation used to describe the time evolution of the state is

$$\frac{dx}{dt} = T(x, v, w, t) = \begin{bmatrix} x_4(t) \\ x_5(t) \\ x_6(t) \\ \frac{v_1(t)}{x_7(t)} + \sum_{i=1}^{N_b} a_x(\text{body} = i, \text{time} = t, x_{1:3}) \\ \frac{v_2(t)}{x_7(t)} + \sum_{i=1}^{N_b} a_y(\text{body} = i, \text{time} = t, x_{1:3}) \\ \frac{v_3(t)}{x_7(t)} + \sum_{i=1}^{N_b} a_z(\text{body} = i, \text{time} = t, x_{1:3}) \\ \dot{m}(\|v\|, x_{1:3}, t) = \text{mass flow rate} \end{bmatrix} \quad (6)$$

The propellant mass flow rate  $\dot{m}$  is a function of the magnitude of the thrust control vector  $\|v\|$ , and the power currently available from the solar array. The power from the solar array is a function of the distance to the Sun, the non-thruster spacecraft power consumption, and time due to solar array degradation. The DAWN thruster  $I_{sp}$  and efficiency is a function of power input<sup>10</sup>. The mass flow is modeled as a differentiable, parametric fit to the thruster performance data. The parameter  $N_b$  is the number of gravitating bodies that are modeled. The gravitational acceleration vector  $a \equiv (a_x, a_y, a_z)$  resulting from each body is given by a time dependent matrix times the gradient of a harmonic expansion of the gravitational potential,

$$a(r, \lambda, \phi, t) = [Q_{body}](t) \cdot \nabla \left\{ \frac{\mu_{body}}{r} \sum_{n=0}^{N_{ex}} \sum_{m=0}^n \frac{R_{body}^n}{r^n} P_{nm}(\sin(\phi))(C_{nm} \cos(m\lambda) + S_{nm} \sin(m\lambda)) \right\} \quad (7)$$

where  $[Q_{body}](t)$  is a rotation matrix from the body fixed rotating frame of the body to an inertial (non-rotating) frame,  $\mu_{body}$  is the gravitational constant of the body,  $r$  is the scalar radius vector from the body center of mass to the spacecraft,  $R_{body}$  is the semi-major axis of the body's ellipsoid used in the expansion,  $P_{nm}$  are the associated Legendre polynomials of degree  $n$  and order  $m$ ,  $\lambda$  is the body fixed longitude of the spacecraft, and  $\phi$  is the body fixed latitude of the spacecraft.  $C_{nm}$  and  $S_{nm}$  are the harmonic expansion constants. The parameter  $N_{ex}$  is the order of the harmonic

expansion. The SDC algorithm was implemented using full second order analytic derivatives (in both time and space) of the harmonic expansion (7).

Given an initial orbital state near an asteroid, the problem is to find the optimal time varying thrust  $v(t)$  and static control parameters  $w$  such that the square of the propellant mass is minimized:

$$\text{Objective : minimize (propellant mass)}^2 \equiv \min_{v,w} (\Gamma_7(w) - x_7(t_f))^2 \quad (8)$$

where  $\Gamma_7(w)$  is the seventh component of the initial state corresponding to the initial spacecraft mass and  $x_7(t_f)$  is the final spacecraft mass. The functions  $F$  and  $G$  in equation (1) are selected to be  $F = 0$  and  $G_1 = (\Gamma_7(w) - x_7(t_f))^2$  (in this application,  $N = 1, t_1 = t_f$ ). The propellant objective is squared to eliminate the incentive to run time backwards and obtain negative propellant masses.

In the numerical applications to follow, the initial state is a given orbit determined by fixed instantaneous classical orbital elements ( $\Gamma(w) =$  pre-specified, fixed state).

### Final State Targeting

The final orbital state constraint used in this analysis has the form of a vector function of the final time and state,  $x$ , that must be equal to, or less than or equal to, a vector constant:

$$\text{Terminal condition : } \Psi(x(t_f), t_f) = \text{or } \leq \text{ vector constant} \quad (9)$$

Constraints of this form translate to a surface or a volume in state space. When constraints of the type (9) are included in the optimal control formulation, the optimal solution's final state will end up on the surface or in the volume.

An example of a function  $\Psi$  is an orbit plane constraint. The final orbital plane can be selected by requiring the orbital angular momentum direction to be parallel to a given constant unit vector  $\hat{h}$ :

$$\frac{(x_{1:3}(t_f) - X_{body}(t_f)) \times (x_{4:6}(t_f) - V_{body}(t_f))}{\|(x_{1:3}(t_f) - X_{body}(t_f)) \times (x_{4:6}(t_f) - V_{body}(t_f))\|} \cdot \hat{h} = 1, \quad (10)$$

where  $X_{body}(t_f)$  and  $V_{body}(t_f)$  are the body's center of mass position and velocity respectively at the final time  $t_f$ . Other constraints were constructed for final orbit instantaneous eccentricity, semi-major axis, longitude of the ascending node etc.

Choosing meaningful terminal constraints for asteroid orbits is not straight forward. The usual constants of motion in the two-body problem like eccentricity, argument of periapsis, etc. do not have analogies in the general asteroid problem. In general, there are no constants of the motion other than total system energy and angular momentum. Targeting instantaneous quantities (like eccentricity) may lead to undesirable local minima because the eccentricity of an uncontrolled orbit around an asteroid may oscillate wildly during each orbit revolution and body rotation. In general, there will be at least one local minima for each feasible number of orbital revolutions used to achieve a specific transfer, and possibly many more. Some of the target orbital states selected in this research were chosen to have relatively stable elements to minimize the aforementioned problem. Such orbits are similar to those that would be selected for science operations. The method used to solve the optimal control problem will admit any differentiable function (9) as a target, so targeting quantities other than instantaneous classical orbital elements can be accommodated.

Other (non-terminal state) constraints in the optimal control formulation include a maximum thrust limit based on the power available, and a minimum allowed close approach distance to each body.

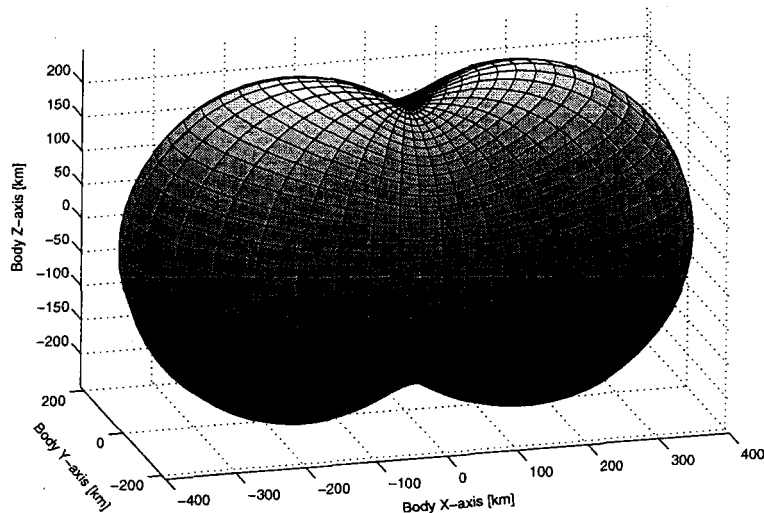


Figure 1: The hypothetical asteroid Peanut.

## RESULTS

A hypothetical dumbbell-like asteroid named “Peanut” was invented for the purpose of studying optimal low-thrust transfers. The asteroid’s shape is plotted in Figure 1. A gravity field for Peanut was computed to tenth order assuming that Peanut has a constant density of  $2.65 \frac{gm}{cm^3}$  (this particular density gives Peanut the same gravitational constant as the asteroid Vesta:  $17.8 \frac{km^3}{s^2}$ ). Fields for Peanut of order  $>10$  were computed, but these fields did not significantly alter solutions. Peanut was constructed to be representative of a coalesced binary asteroid. The maximum extent of Peanut in the X, Y, and Z directions are 400 km, 217.7 km, and 248.8 km respectively. The formula used for Peanut’s surface is

$$radius = 200 + 200 \times |\cosine(longitude)^2 \times cosine(latitude)^{1.2}| [km]. \quad (11)$$

### Orbital Transfers Around Peanut

A series of optimal low-thrust transfers around Peanut were computed. In all cases, the trajectory was constrained to stay above a radius of 430 [km] from Peanut’s center of mass. This constraint ensures that the harmonic expansion for Peanut’s gravity remains convergent and provides a margin of safety of 30 [km] to avoid collisions. If a different gravity model like that of *Weeks and Miller, 2002*<sup>11</sup> was used in place of a harmonic expansion, then optimal trajectories could be obtained inside the of 400 [km] maximum body radius. The spacecraft orbiting Peanut has an initial mass of 500 [kg] with thrusters each producing 122.5 mN with a specific impulse of 3000 seconds. These engine values correspond to an ion engine operating with 2.5 kW of power with an efficiency of 72.1% - a little more efficient than the NSTAR<sup>10</sup> thruster used on NASA’s Deep Space One mission. Peanut is assumed to rotate once every 5.3421 hours (the same as Vesta).

Polar circular to polar circular transfers were investigated first. Polar orbits are scientifically valuable because of surface converge. Near circular, polar orbits below 750 [km] mean radius are unstable so initial and final polar orbits were selected above or at 750 [km]. Of course, nothing prevents intermediate orbits from being below the stability limit. The approximate radius of the 1:1 resonance (spacecraft revolves once for each body rotation) is 550 km for both Vesta and Peanut. Since the lower limit for initial and final orbits is 750 km, The computed transfers will not necessarily pass through the 1:1 resonance. Both the 1:1 and 2:1 resonance can result in strong and interesting perturbations. Polar orbits are stable well below 550 km at Vesta, so the effect of a 1:1 resonance will be explored later in the paper.

Table 1 summarizes several optimized polar to polar transfers. The column under “Rev.s” is

the total number of revolutions completed in 6 days. The column under “ $N_t$ ” is the number of 122.5 mN thrusters used. The column under “Ref #” is a trajectory reference number. All polar to polar transfers allow a maximum flight time of 6 days. The computed inward bound transfers demonstrate the existence of different local minima using different numbers of revolutions (trajectories 2 and 3). The optimization leading to trajectory 2 used an initial guess of no thrusting (1.6816 revolutions). Trajectory 3 was obtained from an initial guess that thrust opposite the body relative velocity vector (5.3136 revolutions). The existence of multiple minima is expected due to oscillations in the targeted classical orbital elements. If classical elements are targeted, it is clear that multiple optimizations using different numbers of revolutions in the initial guess are required to find the best minima. Trajectory number 1 (top row of Table 1) is the result of solving the identical problem that trajectories 2 and 3 solve except a point mass model is used. Comparing trajectories 1 and 3 indicate the propellant can be reduced when the full gravity model is used.

Table 1  
OPTIMAL TRANSFERS BETWEEN POLAR ORBITS

Transfer Type	Propellant Usage [kg]	Time of Flight [d]	Rev.s	$N_t$	Gravity model	Ref #
Inward Bound Transfers						
3500 → 1000 km circ.	1.0074	6.000	5.8757	1	point	1
3500 → 1000 km circ.	1.1168	6.000	3.3543	1	10x10	2
3500 → 1000 km circ.	0.9790	5.904	5.7662	1	10x10	3
1000 → 750 km circ.	0.3165	5.616	11.1105	1	10x10	4

Transfers from circular polar to circular equatorial orbits require large plane changes. Point mass solutions for circular to circular plane change transfers first increase eccentricity, then change plane near apoapsis (where it is easiest,) and finally reduce eccentricity. Table 2 summarizes several optimized polar to equatorial transfers. All transfers using 4 thrusters or 2 thrusters allow a maximum flight time of 6 days or 12 days respectively. An optimal trajectory treating Peanut as a point mass was computed (trajectory 5.) The point mass solution can be compared to the 10x10 gravity solution (trajectory 6.) The 10x10 gravity solution requires less propellant. This indicates SDC is exploiting the non-spherical gravity. Figure 3 compares the time evolution of periapsis, apoapsis, and inclination for the point mass and 10x10 gravity trajectories. Both the point mass and 10x10 gravity solutions follow the same basic pattern: increase eccentricity, perform plane change, and then reduce eccentricity. What is different about the 10x10 gravity case is that it achieves useful changes in apoapsis without thrusting (a gray background in Figure 3 implies thrusting.) The point mass solution uses 13 thrust arcs whereas the 10x10 gravity solution uses only 10 thrust arcs. The close approaches to the asteroid are evident by large oscillations in the orbital elements in the bottom plot of Figure 3. Figure 2 compares the appearance of point mass and 10x10 gravity trajectories (trajectories 5 and 6.)

A simple understanding of optimal transfers in non-spherical gravity can be constructed from a classical elements viewpoint. An optimal trajectory can exploit non-spherical gravity most efficiently during close approaches when both radial and non-radial gravity perturbations are largest. Close approaches are characterized by relatively large velocities. Only some elements can be efficiently changed when the velocity is large. Therefore, optimal trajectories will phase close approaches to achieve large changes in elements like apoapsis, semi-major axis, and/or eccentricity. This is clearly visible in Figure 3. An optimal trajectory will use non-spherical gravity to indirectly change elements like inclination by increasing apoapsis so the change in inclination can be achieved efficiently using thrust when far from the body.

Table 2  
OPTIMAL TRANSFERS BETWEEN POLAR AND EQUATORIAL ORBITS

Transfer Type	Propellant Usage [kg]	Time of Flight [d]	Rev.s	$N_t$	Gravity model	Ref #
Polar to Retrograde equatorial transfers						
1200 → 1200 km circ.	2.6124	6.000	8.0130	4	point	5
1200 → 1200 km circ.	2.4802	5.928	8.1458	4	10x10	6
1200 → 1200 km circ.	2.5618	11.177	16.6521	2	10x10	7
Polar to posigrade equatorial transfer						
1200 → 1200 km circ.	2.5736	11.863	17.0143	2	10x10	8

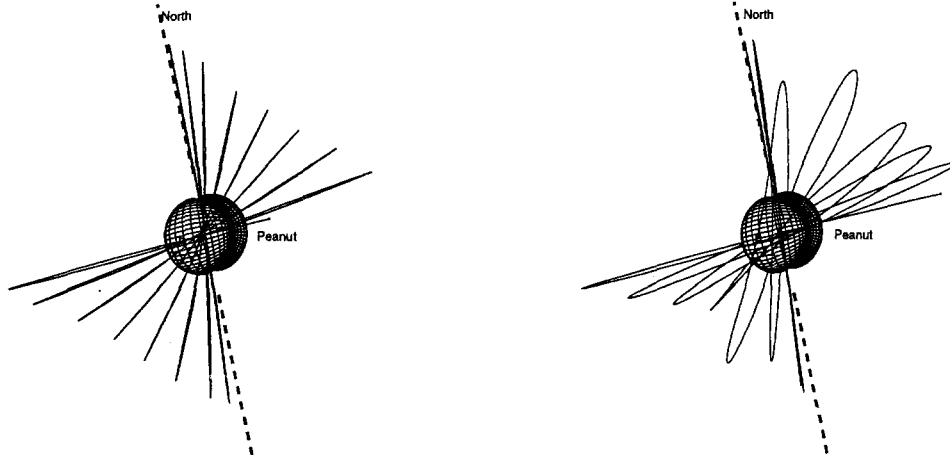


Figure 2: Trajectories 5 and 6 viewed along the initial and final orbit planes. Both trajectories are transfers from 1200 km circular polar orbit to 1200 km circular retrograde orbit around the asteroid Peanut. The trajectory on the left is based on a point mass model, the trajectory on the right is based on the 10x10 gravity model.

Figure 4 is a plot of the instantaneous periapsis, apoapsis, and inclination as a function of time for an optimal trajectory from 1200 km circular polar orbit to 1200 km circular retrograde orbit using 2 thrusters (trajectory 7). This trajectory requires more time than the 4 thruster cases (trajectories 5 and 6), but shows the same characteristics as the higher thrust solutions. The optimal trajectory uses non-spherical gravity to indirectly change inclination by increasing apoapsis at during close approach so inclination change can be achieved efficiently using thrust far from the body.

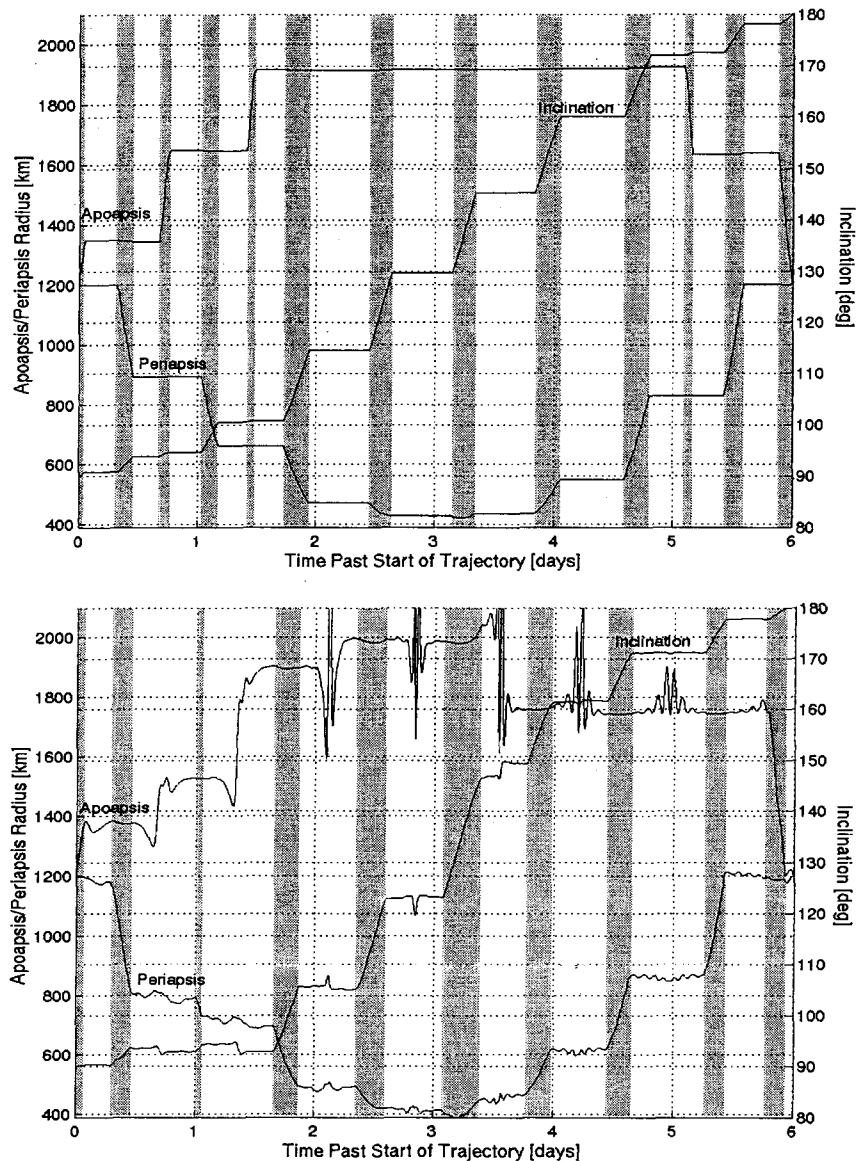


Figure 3: Instantaneous periapsis, apoapsis, and inclination as a function of time for optimal trajectories from 1200 km circular polar orbit to 1200 km circular retrograde orbit around the asteroid Peanut (trajectories 5 and 6). The trajectory represented in the top plot is based on a point mass model. The trajectory represented in the bottom plot is based on a 10x10 gravity model. Gray regions indicate when thrusters are operating.

### Orbital Transfers Around Vesta

The asteroid Vesta is the first target for the DAWN discovery mission. Science orbits at Vesta will all be polar. One required transfer at Vesta is from an initial polar orbit with a mean radius of 950 kilometers to a final polar orbit of 375 kilometers with a plane change of 24 degrees. The plane change is required to maintain optimal Sun-surface view angles and avoid passing into eclipse. Optimal transfers between these orbits were computed based on increasingly complex gravity models for Vesta: point mass model, J2 model, 2X2 model, 4X4 model, and a 20x20 model. The transfer requires more than 100 orbital revolutions for all models. A flight time limit of 25 days was required.

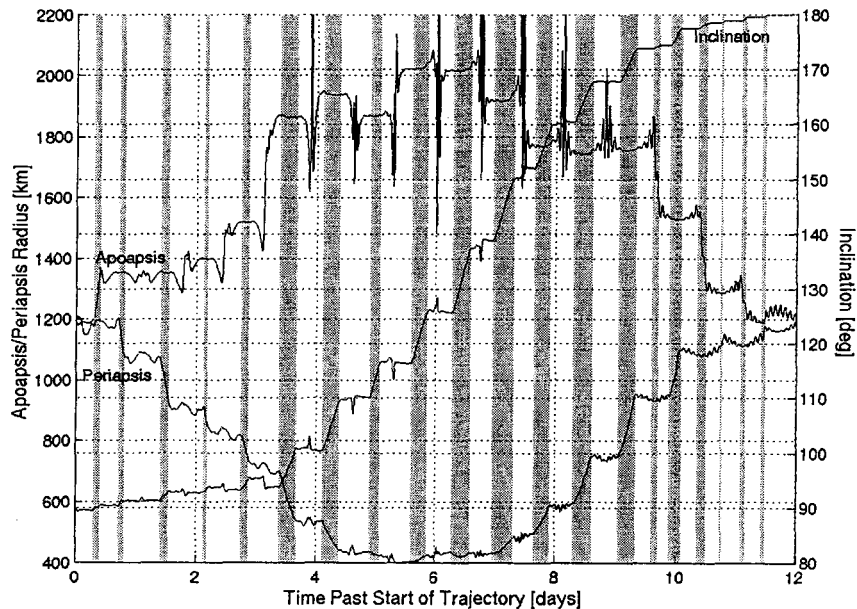


Figure 4: Instantaneous periapsis, apoapsis, and inclination as a function of time for an optimal trajectory from 1200 km circular polar orbit to 1200 km circular retrograde orbit using 2 thrusters (trajectory 7). This trajectory is based on the 10x10 gravity model. Gray regions indicate when thrusters are operating.

The spacecraft power budget and thruster performance are the same as those used for DAWN mission design.

The results for Vesta are summarized in Table 3. Vesta's rotational period is 5.3421 hours. The 1:1 resonance (spacecraft period = 5.3421 hours) corresponds to a circular orbit radius of 550 km. Therefore, all transfers must pass through the 1:1 resonance. The 1:1 resonance has no effect in the point mass and J2 gravity models (trajectories 9 and 10 in Table 3). Once tesseral and sectoral harmonic terms are included (2X2 gravity field and higher) then the 1:1 and other resonances become important.

It turns out that the transfer is infeasible in the point mass model (trajectory 9). The plane change and radius change cannot be accomplished in 25 days. The solution in Table 3 represents a minimization of the infeasibilities: the semi-major axis ends up 26.7 km too high and the orbital plane ends up 7.9 degrees away from the target change of 24 degrees.

If Vesta's J2 ( = .04078055 normalized) is included in the gravity model, then the transfer becomes feasible (trajectory 10). The oblateness of Vesta can be used to precess the longitude of the ascending node when the orbit is not polar. The optimal trajectory moves the inclination away from 90° to precess the ascending node, then returns the inclination to 90° as expected (see the top plot in Figure 5).

Table 3  
VESTA OPTIMAL TRANSFERS

Transfer Type	Propellant Usage [kg]	Time of Flight [d]	Rev.s	Gravity model	Ref #
950 → 375 km circ.	3.2190*	25.0000*	103.2735*	point	9
950 → 375 km circ.	2.3248	24.9750	114.2145	J2	10
950 → 375 km circ.	2.1252	24.8125	113.8165	2X2	11
950 → 375 km circ.	2.0738	22.1821	113.3495	4X4	12
950 → 375 km circ.	2.1277	22.1915	113.6058	20x20	13
950 → 375 km circ.	2.6312	24.9500	123.8786	20x20	14

\* The radius and plane change cannot be completed in 25 days for the point mass case, therefore the transfer is infeasible. These values correspond to a minimization of infeasibilities

The spin of Vesta becomes important when a full 2X2 gravity model is used (trajectory 11). The second order tesseral and sectorial terms create a sensitivity to the rotation of Vesta. In particular, the 1:1 resonance becomes very important. The lower half of Figure 5 provides a plot of instantaneous inclination and longitude of the ascending node as a function of time for the optimal trajectory in the 2X2 field. The tesseral and sectorial terms can be used to reduce propellant mass and flight time significantly over using the J2 term only. There is a long coast through the 1:1 resonance (white area on the bottom plot of Figure 5). SDC optimization has found an orbital state that uses the 1:1 resonance to achieve a significant change in both the inclination and longitude of the ascending node without thrusting.

Using a 4X4 field to represent Vesta's gravity allows SDC to find an even more efficient transfer (trajectory 13). The trajectory in the 4X4 field has an additional feature of interest below the 1:1 resonance. The top half of The trajectory uses the 3:2 resonance to rapidly alter inclination near days 19 and 20. Figure 6 provides a plot of instantaneous inclination and longitude of the ascending node for the optimal trajectory in the 4X4 field.

The largest gravity model used, a 20X20 field, did not significantly change the character of the transfer from that of the 4X4 model (compare the top and bottom plots in Figure 6). However, as with the hypothetical asteroid Peanut, the number of revolutions in the initial guess will dictate the local minima obtained. Comparison of trajectories 13 and 14 in Table 3 indicate that different local minima associated with different numbers of total revolutions result in very different performances. Trajectory 13 requires 19% less propellant and 11% less flight time than trajectory 14. The best procedure to explore the complex-dynamical space of optimal trajectories is to compute optimal trajectories using different numbers of revolutions in each initial guess. The range in the feasible number of revolutions for any particular transfer cannot be a large fraction of the total number of revolutions, so the search will be small. Perhaps a better approach is to adopt orbital targeting parameters which do not oscillate in uncontrolled orbits.

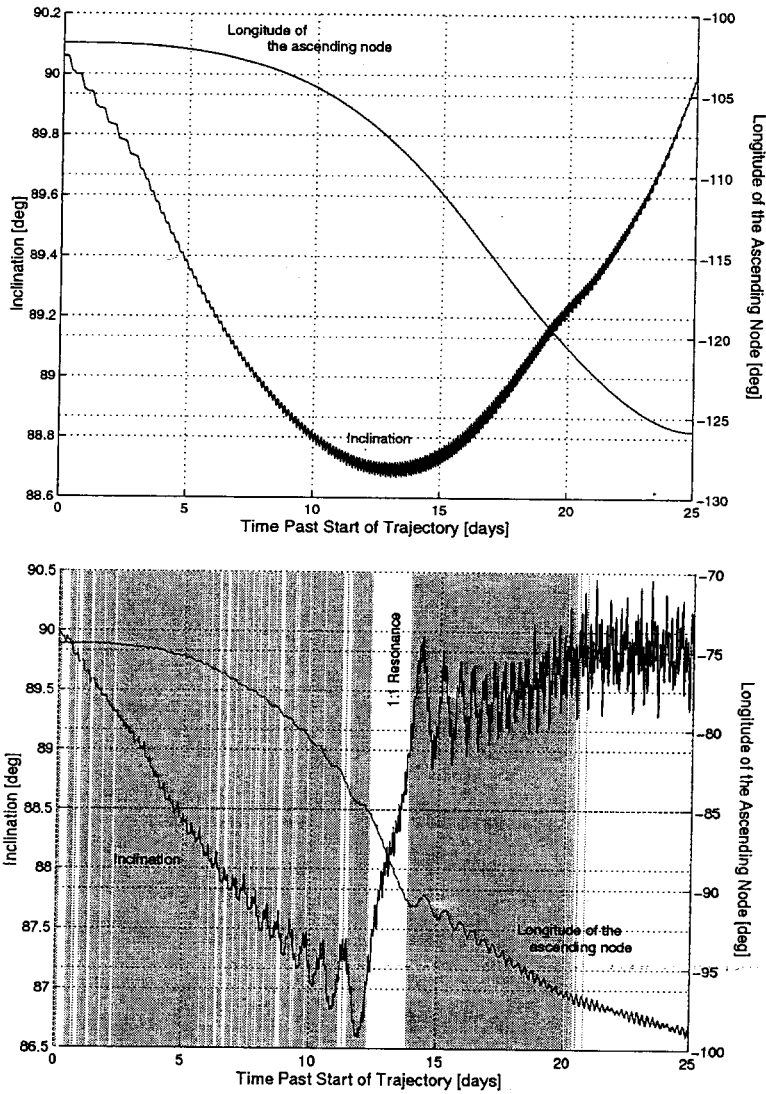


Figure 5: Instantaneous inclination and longitude of the ascending node as a function of time for an optimal Vesta transfer based on a gravity model including only a Keplerian-term and a J2 term (trajectory 10) top plot, and based on a full 2X2 gravity model (trajectory 11) bottom plot. Gray regions indicate when thrusters are operating.

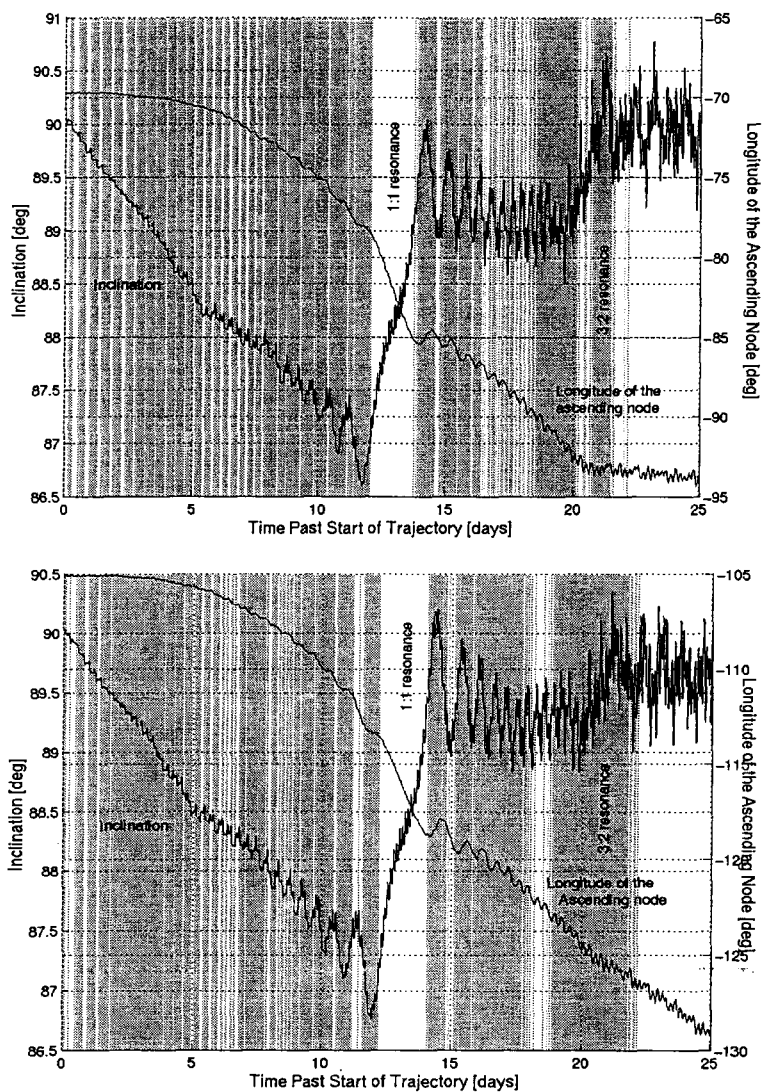


Figure 6: Instantaneous inclination and longitude of the ascending node as a function of time for an optimal Vesta transfer based on a 4X4 gravity model (trajectory 12) top plot, and based on a 20X20 gravity model (trajectory 13) bottom plot. Gray regions indicate when thrusters are operating.

Figure 7 presents a face-on view of the optimal 20X20 gravity field transfer (trajectory 14). The optimal transfer actually spends time at lower altitudes than the final target altitude in order to achieve the most efficient plane change. The transfer ends by rising back up to the target altitude. Figure 8 presents a polar view of the optimal transfer. The maximum rates of plane change occur near the 1:1 and the 2:1 resonances of the spacecraft orbital period versus the rotational period of Vesta. Some plane change also occurs near the 3:2 resonance. A minimum flyby radius constraint must be active to avoid impact. This is due to the ease of plane change at very low altitudes (near the 2:1 resonance). Figure 9 is a plot of the progression of the mean orbital period during the transfer. Note the rapid decline in the period (and hence altitude) when the spacecraft orbital period is near Vesta's rotational period (1:1 resonance). Near the 1:1 resonance, angular momentum can be efficiently transferred from the spacecraft orbit to the rotation of Vesta. Also, note the excursion of the mean period below the target period to the 2:1 resonance. The 2:1 resonance is where the greatest plane change rate occurs in the transfer.

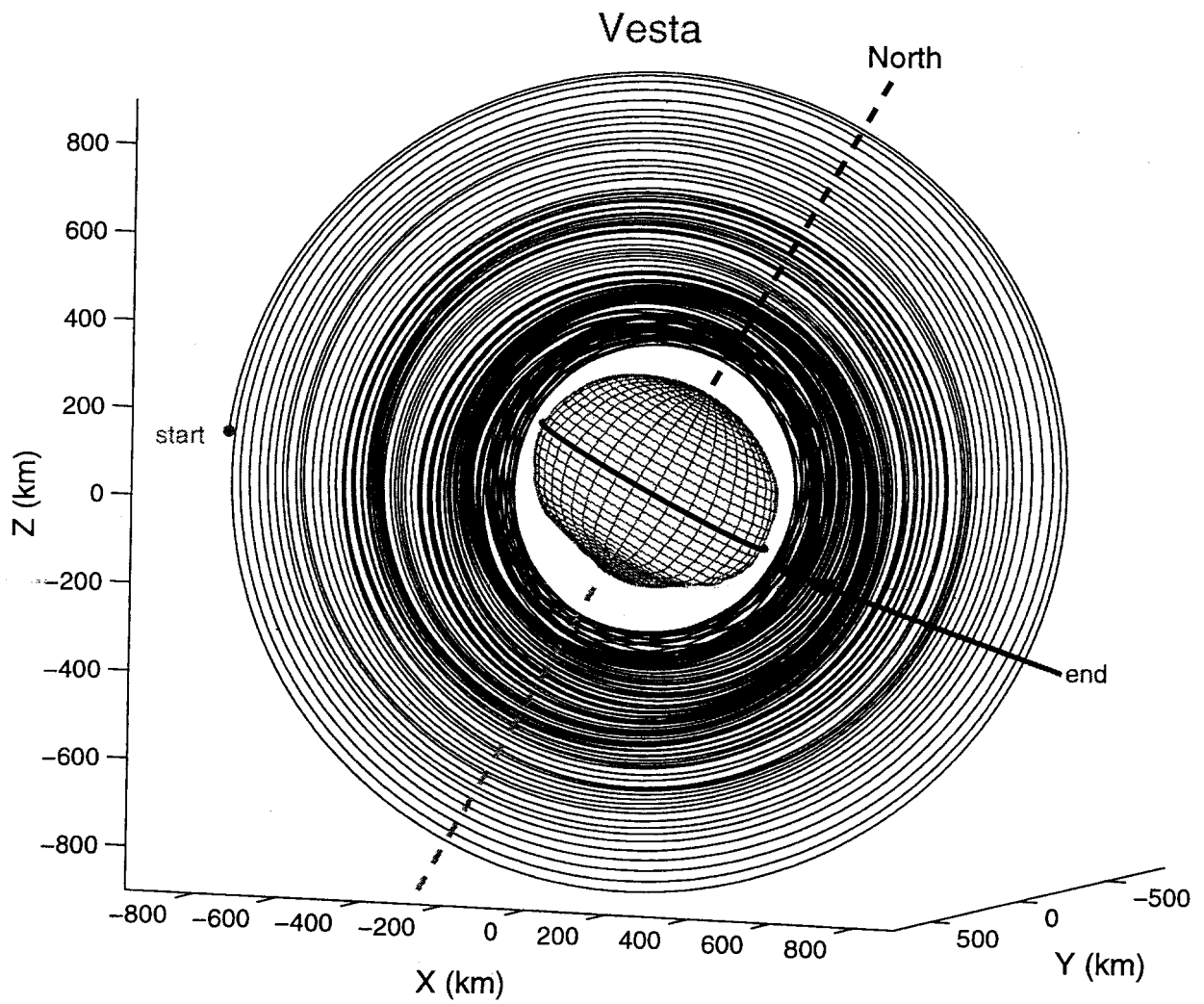


Figure 7: SDC Optimal trajectory from high Vesta polar orbit to low Vesta polar orbit with a plane change of 24 degrees based on the 20X20 gravity model (trajectory 14).

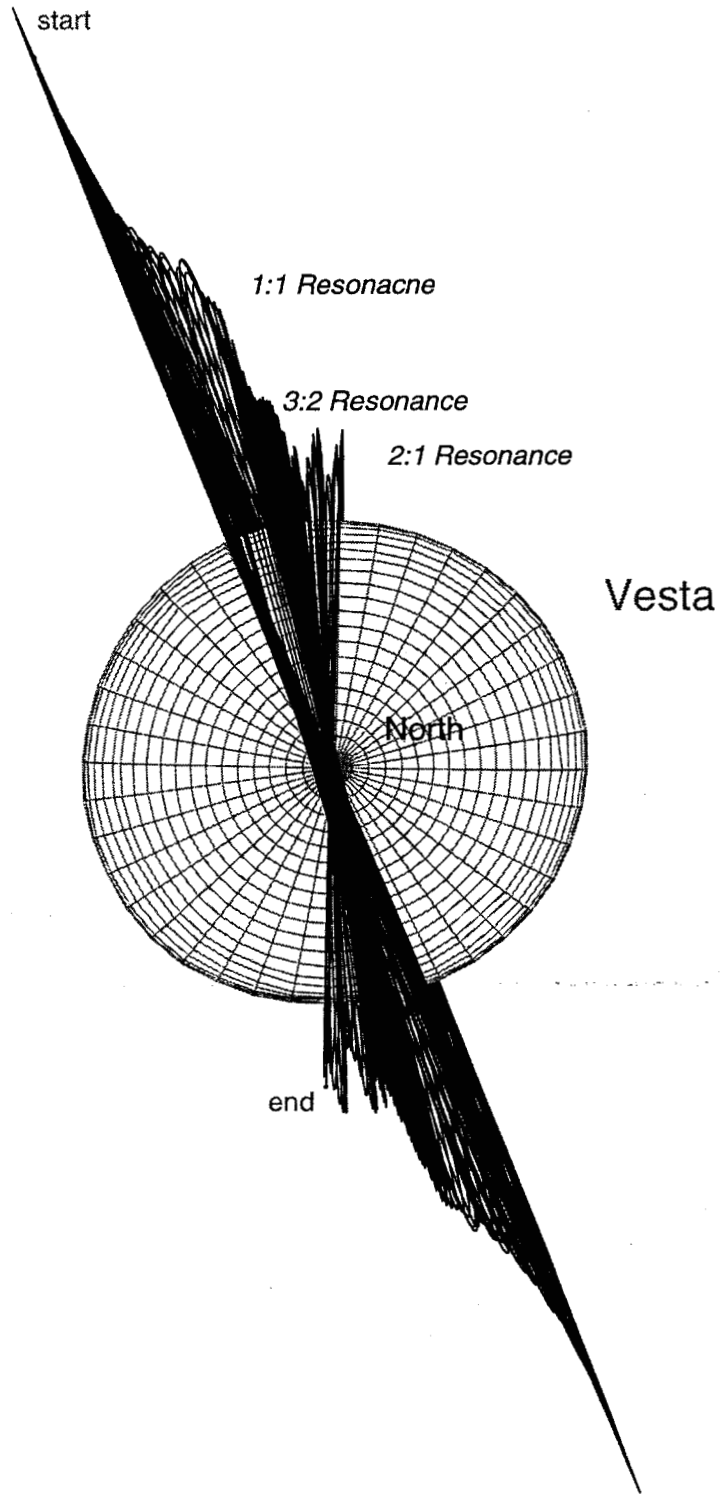


Figure 8: Polar view of SDC Optimal trajectory from high Vesta polar orbit to low Vesta polar orbit with a plane change of 24 degrees based on the 20X20 gravity model (trajectory 14).

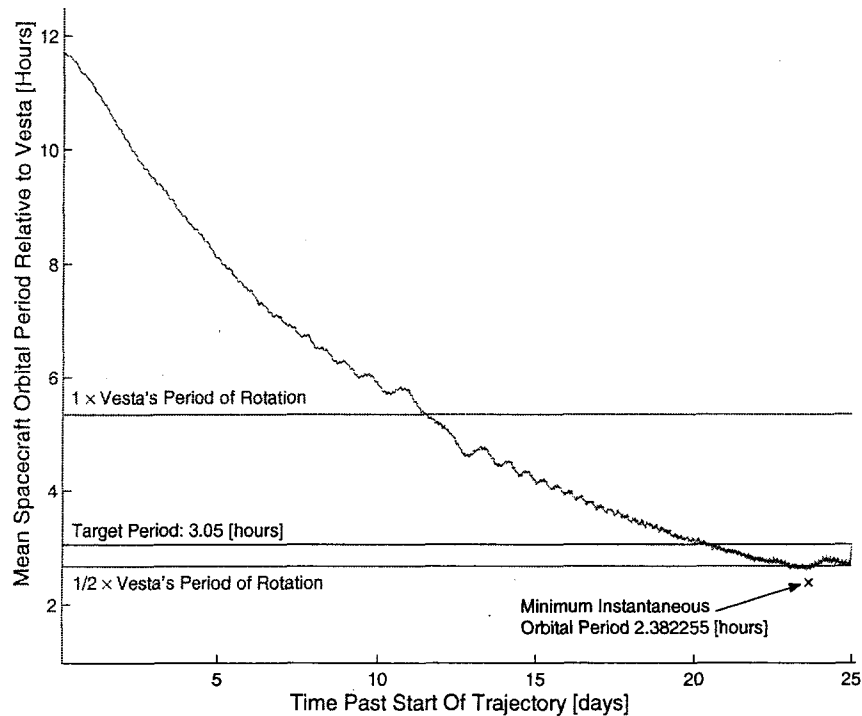


Figure 9: The mean orbital period of the high Vesta polar orbit to low Vesta polar orbit trajectory based on the 20x20 gravity model (trajectory 14). The instantaneous orbital period is moving average over a single revolution.

## SUMMARY AND CONCLUSIONS

An optimal control problem is formulated to minimize the propellant required to achieve an arbitrary orbital transfer around an asteroid. The resulting trajectories use an optimal sequence of stable and unstable orbital states to achieve the desired end state. The optimal sequence of stable and unstable orbital states occur during coasting (thrust off) phases. Since the mathematical objective is to minimize propellant usage, thrusting represents transfers between *adjacent* stable/unstable orbital states. Therefore, the goal of finding and stringing together highly efficient stable/unstable orbital states to reach some goal can be achieved in a single optimization step.

In order for an optimal control approach to work, the optimal control formulation must not omit any of the dynamical complexity of the problem. The gravitational field cannot be simplified. A highly robust optimization method is required. The optimization algorithm called Static/Dynamic Control was selected due to its unusual robustness and ability to solve highly nonlinear dynamic problems. SDC is well suited to explore the optimal trajectories that exist in the asteroid orbit problem. SDC does not require a good guess to begin the optimization. This feature that can be used to explore the optima space of transfers around asteroids.

An understanding of optimal transfers in non-spherical gravity can be constructed from a classical elements viewpoint. An optimal trajectory can exploit non-spherical gravity most efficiently during

close approaches when both radial and non-radial gravity perturbations are largest. Close approaches are characterized by relatively large velocities. Elements like apoapsis, eccentricity, and semi-major axis can be efficiently changed when the velocity is large. Therefore, optimal trajectories will phase close approaches to achieve large changes in elements like apoapsis. An optimal trajectory will use non-spherical gravity to indirectly change elements like inclination (which are best changed far from the body) by increasing apoapsis so the change in inclination can be achieved efficiently using thrust.

## ACKNOWLEDGEMENT

The research described in this paper was carried out at the Jet Propulsion Laboratory, California Institute of Technology, under contract to the National Aeronautics and Space Administration. The author gratefully acknowledges contributions from both James Miller for a computer code that can compute a gravitational harmonic expansion for arbitrary shaped objects, and James Evans for providing a code that computes second order spatial derivatives of a harmonic expansion.

## REFERENCES

1. Kechichian, J. A., "Minimum-Time Constant Acceleration Orbit Transfer with First Order Oblateness Effect," *Journal of Guidance, Control, and Dynamics*, Vol. 23, No. 4, 2000, pp. 595-603.
2. Lara, M., and Scheeres, D. J., "Stability Bounds for Three-Dimensional Motion Close to Asteroids," *Journal of the Astronautical Sciences*, Vol. 50, No. 4, October-December 2002, pp. 389-409.
3. Koon, W. S., Marsden, J. E., Ross, S. D., and Lo, M. W., "Constructing a Low Energy Transfer Between Jovian Moons," *Contemporary Mathematics*, Vol. 292, 2002, pp. 129-145.
4. Whiffen, G. J., "Static/Dynamic Control for Optimizing a Useful Objective," United States Patent No.: 6,496,741, Issued December 17, 2002, Filed March 25, 1999.
5. Whiffen, Gregory J., and Sims, J. A., "Application of a Novel Optimal Control Algorithm to Low-Thrust Trajectory Optimization," Paper AAS 01-209, AAS/AIAA Astrodynamics Specialist Conference, Santa Barbara, California, February 11-14, 2001.
6. Whiffen, G. J., and Sims, J. A., "Application of the SDC Optimal Control Algorithm To Low-Thrust Escape and Capture Trajectory Optimization," Paper AAS 02-208, AAS/AIAA Space Flight Mechanics Conference, San Antonio, Texas, USA, January 27-30, 2002.
7. Whiffen, G. J., and Sims, J. A., "Application of the SDC Optimal Control Algorithm To Low-Thrust Escape and Capture Including Fourth Body Effects," 2<sup>nd</sup> International Symposium on Low Thrust Trajectories, Toulouse, France, June 18-20, 2002.
8. Whiffen, G. J., "An Investigation of a Jupiter Galilean Moon Orbiter trajectory," Paper AAS03-544, AAS/AIAA Astrodynamics Specialists Conference, Big Sky, Montana, USA, August 3-7, 2003.
9. Sims, J. A., Whiffen, G. J., Finlayson, P. A., Petropoulos, A. E., "Low-Thrust Orbit Transfer Around Minor Planets," Paper AAS 02-139, AAS/AIAA Space Flight Mechanics Conference, San Antonio, Texas, USA, January 27-30, 2002.
10. Polk, J. E., Anderson, J. R., Brophy, J. R., Rawlin, V. K., Patterson, M. J., and Sovey, J. S., "The Effect of Engine Wear on Performance in the NSTAR 8000 Hour Ion Engine Endurance Test," Paper AIAA 97-3387, 33rd AIAA/ASME/SAE/ASEE Joint Propulsion Conference and Exhibit, Seattle, WA, July 6-9, 1997.
11. Weeks, C., and Miller, J. K., "A Gravity Model For navigation Close to Asteroids and Comets," Paper AAS 02-140, AAS/AIAA Space Flight Mechanics Conference, San Antonio, Texas, USA, January 27-30, 2002.